J Biomol NMR (2011) 51:379–394
DOI 10.1007/s10858-011-9564-7

ARTICLE

Structure, dynamics, and ionization equilibria of the tyrosine residues in *Bacillus circulans* xylanase

Simon J. Baturin · Mark Okon · Lawrence P. McIntosh

Received: 12 August 2011 / Accepted: 26 August 2011 / Published online: 13 September 2011

Abstract We have developed NMR spectroscopic methods to investigate the tyrosines within *Bacillus circulans* xylanase (BcX). Four slowly exchanging buried tyrosine hydroxyl protons with chemical shifts between 7.5 and 12.5 ppm were found using a long-range ^{13}C-HSQC experiment that exploits the $^{3}J_{CH}$ coupling between the ring $^{1}H^{\eta}$ and $^{13}C^{\varepsilon}$ nuclei. The NMR signals from these protons were assigned via ^{13}C-tyrosine selective labelling and a suite of scalar and ^{13}C,^{15}N-filtered/edited NOE correlation spectra. Of the fifteen tyrosines in BcX, only the buried Tyr79 and Tyr105 showed four distinct, rather than two averaged, signals from ring ^{13}C–^{1}H pairs, indicative of slow flipping on the chemical shift timescale. Ring flipping rate constants of $\sim$10 and $\sim$0.2 s^{-1} were measured for the two residues, respectively, using a ^{13}C longitudinal exchange experiment. The hydrogen bonding properties of the Tyr79 and Tyr105 hydroxyls were also defined by complementary NOE and J-coupling measurements. The $^{1}H^{\eta}$ hydrogen–deuterium exchange rate constants of the buried tyrosines were determined from ^{13}C/^{15}N-filtered spectra recorded as a function of pH. These exchange rate constants correspond to estimated protection factors of $\sim 10^{4}$–10^{8} relative to a random coil tyrosine. The phenolic sidechain pK_a values were also measured by monitoring their pH-dependent $^{13}C^{\zeta}$ chemical shifts via $^{1}H^{\varepsilon/\delta}(^{13}C^{\varepsilon})^{13}C^{\zeta}$ correlation spectra. Exposed tyrosines had unperturbed pK_a values of $\sim$10.2, whereas buried residues remained predominantly neutral at or even above pH 11. Combined with selective isotope labelling, these NMR experiments should prove useful for investigating the structural and electrostatic properties of tyrosines in many interesting proteins.

Keywords Glycoside hydrolase · Tyrosine hydroxyl · Protein dynamics · Protein electrostatics · NMR spectroscopy

Introduction

Tyrosine residues play critical structural and functional roles in proteins (Creighton 2010). With both an aromatic ring and an ionizable hydroxyl group, the amphiphatic sidechain of this amino acid can partake in a range of hydrophobic and polar interactions necessary to stabilize the native, folded conformation of a protein or protein complex (Pace et al. 2001). In addition to ligand and substrate binding, the tyrosine phenolic group can also contribute directly to enzymatic catalysis (Holliday et al. 2009), serving as a nucleophile (Watts et al. 2003; Yang 2010), general acid/base (Li et al. 1993; Sun and Toney 1999; Lunin et al. 2004), or redox active centre (Barry and Einarsdottir 2005). Key to all of these roles is the ionization state and hydrogen bonding properties of a given tyrosine. However, unless neutron (Kossiakoff et al. 1990) or very high resolution X-ray diffraction data (Ho and Agard 2008) are available, electron density from a hydroxyl H^{η} is typically not observed in a crystallographically-determined protein structure. Similarly, although tyrosines have been well studied since the earliest days of protein NMR spectroscopy, the hydroxyl proton is rarely detected

Electronic supplementary material The online version of this article (doi:10.1007/s10858-011-9564-7) contains supplementary material, which is available to authorized users.

S. J. Baturin · M. Okon · L. P. McIntosh (✉)
Department of Biochemistry and Molecular Biology, Department of Chemistry, and Michael Smith Laboratories, University of British Columbia, Life Sciences Centre, 2350 Health Sciences Mall, Vancouver, BC V6T 1Z3, Canada
e-mail: mcintosh@chem.ubc.ca

via this technique due to rapid hydrogen exchange with solvent water (Liepinsh et al. 1992; Liepinsh and Otting 1996). Thus, the functional properties of tyrosine sidechain hydroxyls are more often inferred from physicochemical arguments than from direct experimental measurements.

In this study, we report the detailed characterization of the tyrosines in *Bacillus circulans* xylanase (BcX) using a suite of both established and new NMR methods. This well characterized family 11 glycoside hydrolase (Cantarel et al. 2009) exploits two catalytic glutamic acid residues to hydrolyze xylan via a double displacement retaining mechanism (Miao et al. 1994). Although composed of only 185 amino acids, BcX contains fifteen tyrosines that both contribute to its β-jellyroll fold and line its active site cleft (Wakarchuk et al. 1994; Sidhu et al. 1999). Indeed, carbohydrate-protein interactions are often mediated by the stacking of sugars against aromatic rings. The $^{1}H^{\eta}$ signals of four tyrosines in isotopicically labeled BcX are readily detectable by ^{1}H-NMR methods with filtering against $^{13}C/^{15}N$-bonded protons. Using the same approach to measure tyrosine hydrogen/deuterium exchange (HX) kinetics, we found that the hydroxyls from these residues are protected against exchange by $\sim 10^{4}$–10^{8} fold relative to a random coil tyrosine due to their burial within the well structured core of BcX. Two of these tyrosines also undergo slow ring flipping on the seconds timescale, thus allowing their $^{1}H^{\eta}$ groups to be positioned within the crystal structure of BcX using complementary NOE and J-coupling restraints. This both unambiguously defines their neutral ionization states and hydrogen bonding properties. Finally, the pK_a values of the tyrosines in BcX were determined from their pH-dependent $^{13}C^{\zeta}$ chemical shifts. Three exposed tyrosines have relatively unperturbed pK_a values of $\sim$10.2, whereas the remainder remain predominantly neutral at or even above pH 11. Collectively, these results both shed new insights into the structure and stability of BcX, and illustrate routes for the characterization of tyrosines in proteins by NMR spectroscopy.

Materials and methods

Protein expression and purification

The expression and purification of BcX has been described previously (Joshi et al. 2001). Briefly, *E. coli* BL21(λDE3) cells were transformed with a pET22b(+) vector encoding for BcX and grown at 37°C in LB media or in M9 medium with 1 g/L $^{15}NH_4Cl$ or 1 g/L $^{15}NH_4Cl$ and 3 g/L $^{13}C_6$-glucose (Spectra Stable Isotope) to produce unlabelled or uniformly labelled protein, respectively. BcX, selectively labelled with ^{13}C-tyrosine, was obtained from BL21 cells grown in M9 media containing per litre 25 mg $^{13}C_9/^{15}$N-L-tyrosine (Isotec), 100 mg unlabelled tryptophan, 100 mg unlabelled phenylalanine, and 1 g N-(phosphonomethyl)glycine (Sigma-Aldrich). The latter, also known as glyphosate, inhibits the biosynthesis of aromatic amino acids (Kim et al. 1990). The cells were initially incubated at 37°C, then transferred to 30°C when an OD_{600} of $\sim$0.4 was achieved.

In all cases, at $OD_{600} = 0.6$, protein expression was induced with 1 mM IPTG. The cells were harvested after $\sim$20 h growth at 37°C (or overnight at 30°C for ^{13}C-tyrosine selective labelling), and lysed with a French press in the presence of a protease inhibitor cocktail (Roche Diagnostics). BcX was eluted with a 0–1 M NaCl gradient (10 mM sodium phosphate, pH 6.0) from a 20 mL Hi-Trap SP-Sepharose (GE Healthcare) ion exchange chromatography column. The resulting protein samples were purified further using a HiPrep 16/60 Sephacryl S-100 (GE Healthcare) size-exclusion column equilibrated with 150 mM NaCl, 10 mM sodium phosphate, pH 6.0, and then concentrated with buffer adjustment by ultrafiltration. The final sample concentrations were determined by absorbance spectroscopy using a predicted ε_{280} value of 81,790 M^{-1} cm^{-1}.

NMR spectroscopy

NMR spectra were recorded with Varian Unity 500 MHz and cryoprobe-equipped Inova 600 MHz spectrometers. Data were processed with NMRpipe (Delaglio et al. 1995) and analyzed using Sparky (Goddard and Kneeler 1999). Unless stated otherwise, protein samples were in 10 mM sodium phosphate, pH 6.5, with 5% D_2O lock solvent and at 25°C. The spectral assignments of main chain nuclei were obtained from $^{15}N/^{13}$C-HSQC, HNCACB, CBCA-CONH, HNCO, HN(CA)CO, and ^{15}N-editted TOCSY- and NOESY-HSQC spectra (Sattler et al. 1999), combined with previously reported data for the wild type protein (Plesniak et al. 1996b; Connelly et al. 2000). The signals from tyrosine ^{1}H and ^{13}C nuclei in ^{13}C-Tyr labelled BcX were assigned using a variety of single and multiple bond correlation experiments, presented in the Results section. The pulse sequences for these experiments are given as Supplemental Fig. S1–S8 and are available upon request.

Hydrogen exchange

Tyrosine hydrogen–deuterium exchange rates were measured at 25°C using one-dimensional $^{13}C/^{15}N$-filtered experiments (Supplemental Fig. S1). $^{13}C/^{15}N$-BcX samples ($\sim$500 µL) in 10 mM sodium phosphate, H_2O, were adjusted to a desired pH value, lyophilized, reconstituted in an equivalent volume of D_2O, and immediately placed in the spectrometer. The decay of the tyrosine $^{1}H^{\eta}$ peak

intensity, I_t, was monitored as a function of time. Data were fit to an exponential decay with GraphPad Prism 5, according to the equation:

$$I_t = I_0 e^{-k_{ex}t} + I_\infty$$

where I_o and I_∞ are the initial and final peak intensities, respectively. The sample pH* (i.e., the pH meter reading without correction for the deuterium isotope effect) was measured after completion of the experiment.

Tyrosine ring flipping

The ring flipping rates of Tyr79 and Tyr105 in ^{13}C-tyrosine selectively labelled BcX were measured using the pulse sequence of Farrow et al. (Farrow et al. 1994), modified for an aromatic ^{13}C–^{1}H spin system (Supplemental Fig. S4). The experiment provides both the ^{13}C longitudinal decay (R_1) and conformational exchange rate constants (k) of the non-degenerate $^{13}C^{\varepsilon 1}/^{13}C^{\varepsilon 2}$ or $^{13}C^{\delta 1}/^{13}C^{\delta 2}$ of a given tyrosine ring, detected in the form of a one-bond ^{13}C-HSQC spectrum. These values were extracted by simultaneously fitting time-dependent "auto" ($I_{C_1/H_1}(t)$ and $I_{C_2/H_2}(t)$) and "exchange" ($I_{C_1/H_2}(t)$ and $I_{C_2/H_1}(t)$) peak intensities to the following equations, using GraphPad Prism 5:

$$I_{C_i/H_i}(t) = I_{C_i/H_i}(0) \left(-(\lambda_- - a_i)\, e^{-\lambda_+ t} + (\lambda_+ - a_i)\, e^{-\lambda_- t}\right)/(\lambda_+ - \lambda_-)$$

$$I_{C_i/H_j}(t) = I_{C_i/H_i}(0) \left(-k\, e^{-\lambda_+ t} + k\, e^{-\lambda_- t}\right)/(\lambda_+ - \lambda_-)$$

where

$$\lambda_{+,-} = \frac{1}{2}\left\{(a_1 + a_2) \pm \left[(a_1 - a_2) + 4k^2\right]^{1/2}\right\}$$

and $a_1 = (R_{1,C_1} + k)$ and $a_2 = (R_{1,C_2} + k)$. These expressions follow from those of Farrow et al. (1994) with the simplification of a single rate constant for flipping of the symmetrical ring.

pK_a measurements

Two-dimensional proton-detected $^{1}H^{\varepsilon}(^{13}C^{\varepsilon})^{13}C^{\zeta}$ and $^{1}H^{\varepsilon/\delta}(^{13}C^{\varepsilon/\delta})^{13}C^{\zeta}$ experiments were developed to measure the pK_a of tyrosine residues by monitoring the ionization-sensitive $^{13}C^{\zeta}$ shifts as a function of sample pH value (Supplemental Fig. S5 and S7). Three-dimensional versions of these pulse sequences were also used to facilitate resonance assignments (Supplemental Fig. S6 and S8). Experiments were carried out with ^{13}C-tyrosine selectively labelled BcX in 10 mM sodium phosphate, 5% D_2O at 35°C. The sample pH value was adjusted by the addition of small aliquots of 0.1 mM NaOH. Site-specific pK_a values were obtained by fitting with MatLab the pH-dependent $^{13}C^{\zeta}$ chemical shifts to the equation describing a single titration,

$$\delta_{obs} = \frac{\delta_a 10^{-pH} + \delta_b 10^{-pKa}}{10^{-pH} + 10^{-pKa}}$$

where δ_a and δ_b are the limiting chemical shift values for the conjugate acid and base forms of the tyrosine, respectively. In the case of a partial titration, $(\delta_b - \delta_a)$ was constrained to 9.7 ppm. This value is based on the pH-dependent $^{13}C^{\zeta}$ chemical shifts of free tyrosine in 10 mM sodium phosphate buffer and 5% D_2O, measured from ^{13}C-HMBC spectra (Supplemental Fig. S9) (Bax and Summers 1986).

Results

Detection of tyrosine $^{1}H^{\eta}$ signals

The ^{1}H-NMR spectrum of BcX contains three signals downfield of 11 ppm (Fig. 1a). One of these has been assigned to the nitrogen-bonded $^{1}H^{\varepsilon 2}$ of the buried, neutral His149 (Plesniak et al. 1996a; Connelly and McIntosh 1998). The other two must arise from slowly exchanging oxygen- or less likely, sulfur-bonded protons because they

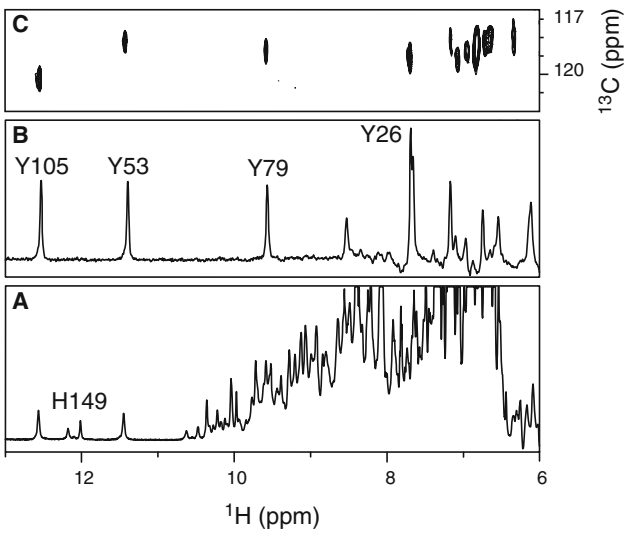

Fig. 1 **a** The ^{1}H-NMR spectrum of ^{13}C/^{15}N-BcX recorded without ^{13}C/^{15}N-decoupling shows two downfield singlets arising from –OH groups. The doublet from the nitrogen-bonded $^{1}H^{\varepsilon 2}$ of His149 is indicated (Plesniak et al. 1996a). **b** The ^{13}C/^{15}N-filtered spectrum of ^{13}C/^{15}N-BcX reveals additional ^{1}H signals originating from oxygen-bonded protons. **c** Four of these signals are assigned to tyrosines based on three-bond $^{1}H^{\eta}$–$^{13}C^{\varepsilon}$ correlations detected in a long-range ^{13}C-HSQC spectrum of BcX selectively labelled with ^{13}C-tyrosine. Additional unassigned peaks in **b** are likely from serine and threonine hydroxyls, and those in **c** arise from multiple-bond correlations between non-labile tyrosine aromatic ring ^{1}H and ^{13}C nuclei. All spectra were recorded at pH 6.5 and 25°C

remain as singlets when BcX is uniformly $^{13}C/^{15}N$-labelled. To confirm this, we recorded the 1D spectrum of $^{13}C/^{15}N$-BcX with filtering against protons bonded directly to ^{13}C and ^{15}N nuclei (Fig. 1b and Supplemental Fig. S1). In addition to the peaks at 12.53 and 11.50 ppm, at least seven more signals were detected downfield of 6 ppm. Based on their chemical shifts, it was reasonable to attribute at least some of these to the tyrosine hydroxyls in BcX. As tabulated in the BioMagResBank (Ulrich et al. 2008), the average tyrosine $^1H^{\eta}$ chemical shift in diamagnetic proteins is 9.33 ppm, compared to 5.34 ppm for serine $^1H^{\gamma}$, 4.96 ppm for threonine $^1H^{\gamma 1}$, 1.94 for cysteine $^1H^{\gamma}$ (BcX is thiol-free), and 9–12 ppm for the rarely observed carboxyl protons of aspartic and glutamic acids.

Four of the signals from -OH groups were unambiguously assigned to tyrosine hydroxyls using a multiple bond ^{13}C-HSQC experiment recorded on a sample of BcX selectively labelled with ^{13}C-Tyr (Fig. 1c and Supplemental Fig. S2). The experiment exploits a modest $^3J_{HC}$ to correlate the $^1H^{\eta}$ and $^{13}C^{\varepsilon}$ of a tyrosine (Werner et al. 1997). Although this scalar coupling is conformationally dependent, the $^1H^{\eta}$ signal of ^{13}C-tyrosine in DMSO is split into a double doublet due to an averaged $^3J_{HC} \sim 5$ Hz with two equivalent $^{13}C^{\varepsilon}$ nuclei. Note that the multiple-bond experiment was recorded using an INEPT 1/4 J transfer delay of n/(2*160 Hz) to minimize signals from tyrosine one-bond ^1H-^{13}C couplings. Due to a balance of transfer versus relaxation, delays of 6.2, 9.4 or 15.6 ms gave similar quality spectra with BcX, with the latter two being optimal at 30 and 37°C, respectively. Weak $^1H^{\eta}$–$^{13}C^{\zeta}$ correlation were also observed due to a small $^2J_{HC}$ (not shown), aiding in the specific assignments of the $^1H^{\eta}$ signals, as outlined below. Although the long-range ^{13}C-HSQC experiment can be recorded using a uniformly ^{13}C-labelled protein sample, identification of the tyrosine signals will be complicated by the presence of numerous 2- and 3-bond correlations between ^{13}C nuclei and various aromatic, indole, imidazole, and amide protons.

Assignment of tyrosine $^1H^{\eta}$ signals

The signals from tyrosine $^1H^{\eta}$ nuclei were assigned using a set of scalar and NOE correlation experiments (Fig. 2 and Supplemental Table S1). Briefly, the chemical shifts of the main chain nuclei of BcX were identified previously using standard methods (Plesniak et al. 1996b; Connelly et al. 2000). The ring $^1H^{\delta}$–$^{13}C^{\delta}$ and $^1H^{\varepsilon}$–$^{13}C^{\varepsilon}$, which give well resolved peaks in a constant-time one-bond ^{13}C-HSQC

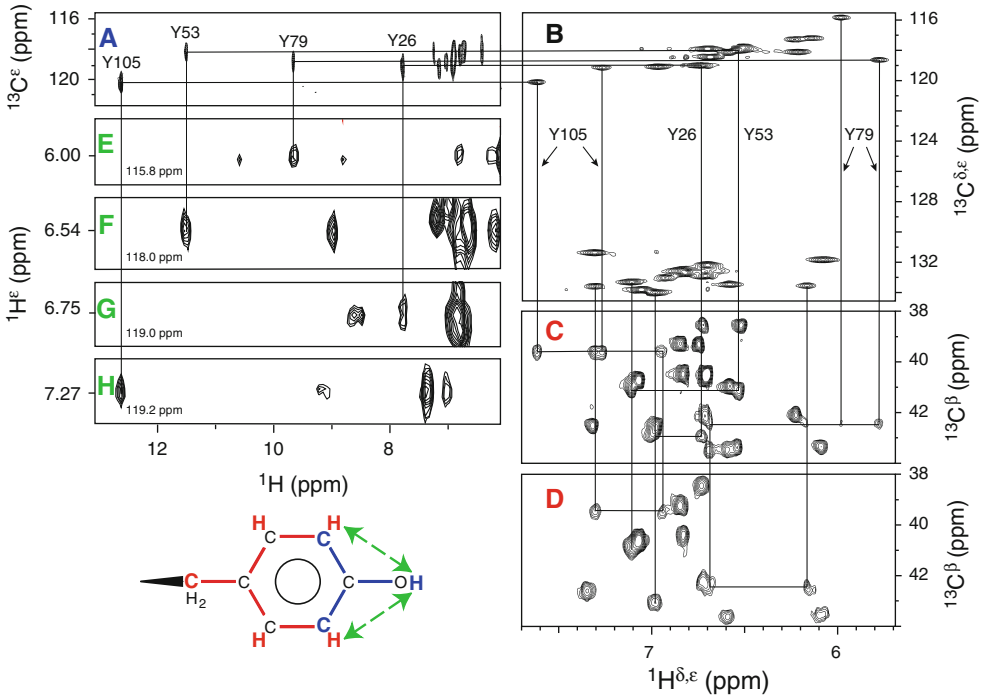

Fig. 2 Signals from the tyrosine $^1H^{\eta}$ nuclei were assigned using **a** a long-range ^{13}C-HSQC spectrum to provide correlations to the $^{13}C^{\varepsilon}$, which were then aligned to a **b** one-bond constant time ^{13}C-HSQC spectrum. The $^1H^{\varepsilon}$–$^{13}C^{\varepsilon}$ and $^1H^{\delta}$–$^{13}C^{\delta}$ peaks in this spectrum were assigned using **c** $C^{\beta}(C^{\gamma}CC\text{-}TOCSY)H^{ar}$ and **d** $C^{\beta}(C^{\gamma}C^{\delta})H^{\delta}$ spectra, which correlate the ring $^1H^{\varepsilon/\delta}$ or $^1H^{\delta}$, respectively, to the $^{13}C^{\beta}$. The assignments were confirmed using a **e**–**h** ^{13}C-edited NOESY-HSQC spectrum, from which ω_1 (horizontal)—ω_3 (*vertical*) strips at the indicated $^{13}C^{\varepsilon}$ chemical shifts are shown. Spectra **a**–**d** were recorded with ^{13}C-Tyr BcX and **e**–**h** with the uniformly labelled ^{13}C-BcX, all at 35°C. For clarity, only peaks from the four tyrosines with detectable $^1H^{\eta}$ are annotated. Complete assignments are given in Supplemental Table S1

spectrum, were linked to the $^{13}C^{\beta}$ using $C^{\beta}(C^{\gamma}C^{\delta})H^{\delta}$ (Yamazaki et al. 1993a) and $C^{\beta}(C^{\gamma}CC\text{-}TOCSY)H^{ar}$ (Löhr et al. 2005; Löhr et al. 2007) (Supplemental Fig. S3) experiments. Knowledge of the $^{13}C^{\varepsilon}$ chemical shifts then allowed the specific assignment of the $^{1}H^{\eta}$ signals detected via $^{1}H^{\eta}$–$^{13}C^{\varepsilon}$ correlations in the long-range ^{13}C-HSQC spectrum of BcX. These assignments were confirmed using a ^{13}C-edited NOESY-HSQC spectrum, which detects NOEs from the $^{1}H^{\eta}$ to the adjacent ^{13}C-labelled $^{1}H^{\varepsilon}$. Additional verification was provided by assigning the $^{13}C^{\zeta}$ signals of the tyrosine rings for pK_a measurements (see below), combined with the observation of weak $^{1}H^{\eta}$–$^{13}C^{\zeta}$ correlations in a long-range ^{13}C-HSQC spectrum (not shown).

The four detected $^{1}H^{\eta}$ signals arise from Tyr26, Tyr53, Tyr79, and Tyr105 (Figs. 1, 2). Of the fifteen tyrosines in BcX, these are the most buried with O^{η} accessible surface areas <1 Å^2 in the static X-ray crystallographic structure of this protein (Fig. 3; Table 1). In addition, each is hydrogen bonded to neighbouring protein atoms and/or bound waters. This of course is expected, since a tyrosine $^{1}H^{\eta}$ must be protected from rapid HX in order to be detected under the conditions used for these measurements.

Tyrosine $^{1}H^{\eta}$ hydrogen exchange kinetics

The HX kinetics of the protected tyrosines in BcX were measured by recording one-dimensional $^{13}C/^{15}N$-filtered spectra immediately after transfer of the $^{13}C/^{15}N$-labelled protein into D_2O buffer (Fig. 4a,b). Fitting of the time-dependent decay of the signals from Tyr26, Tyr53, and Tyr79 yielded the exchange rate constants, k_{ex}, summarized in Fig. 4c. Interestingly, the exchange kinetics of Tyr53 showed little dependence on the pH conditions examined. This is suggestive of an EX1 or open-limited mechanism (Hvidt and Nielsen 1966; Englander and Kallenbach 1983). In contrast, Tyr26 and Tyr79 exhibited pH-dependent HX, indicative of exchange via an EX2 or pre-equilibrium mechanism. Furthermore, both exchanged most slowly around pH* 5–6, which is similar to the pH_{min} ~5.5 reported for an unperturbed tyrosine (Liepinsh et al. 1992; Liepinsh and Otting 1996). Based on an estimated pseudo-first order $k_{predict}$ ~10^3 s^{-1} for the exchange of a free tyrosine hydroxyl under comparable conditions (Liepinsh et al. 1992; Liepinsh and Otting 1996), the protection factors ($k_{predict}/k_{ex}$) of Tyr53, Tyr26, and Tyr79 at pH* 4.3 and 25°C are ~10^6, 10^7, and 10^8, respectively. The effects of possible general base catalysis have been neglected in these approximations.

Although the $^{1}H^{\eta}$ of Tyr105 is detectable in H_2O, its signal was absent immediately after transfer to D_2O under all pH* conditions examined (Fig. 4b). Assuming a dead time of ~180 s between rehydration of the lyophilized sample and recording the first NMR spectrum, this indicates that its $k_{ex} > 0.01$ s^{-1}. In contrast, no transfer of magnetization from H_2O to Tyr105 (or to the other three observable tyrosines) was detected in a one-dimensional CLEANEX experiment (Hwang et al. 1997) with a $^{13}C/^{15}N$-filtered readout (pH 4.5–6.5; not shown). This sets an approximate upper limit of $k_{ex} < 0.1$ s^{-1} for Tyr105, and hence a protection factor within the range of ~10^4–10^5. This limit is also consistent with the requirement that $k_{ex} < {}^{3}J_{CH}$ in order to detect the $^{1}H^{\eta}$ in a long range ^{13}C-HSQC spectrum without significant loss of polarization transfer (Henry and Sykes 1990).

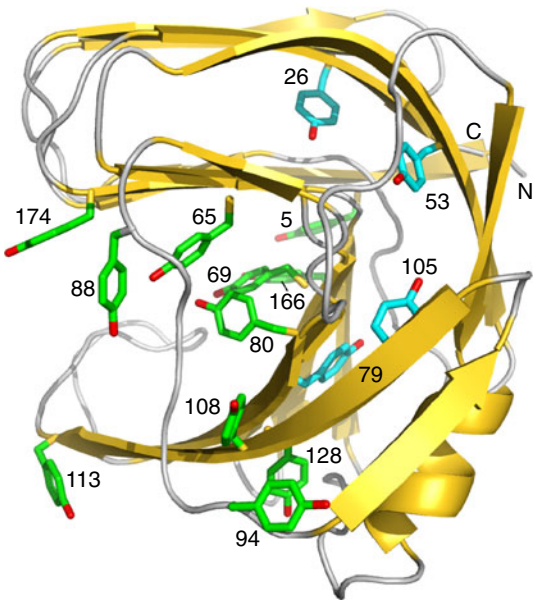

Fig. 3 A ribbon diagram of BcX with all fifteen tyrosines shown in stick format. The four most buried (Tyr26, Tyr53, Tyr79, and Tyr105; cyan) have detectable $^{1}H^{\eta}$ signals. Rendered with PyMol (DeLano 2004) using 1XNB.pdb (oxygen *red*; carbon *cyan* or *green*)

Tyrosine ring flipping

As typically observed with proteins, eleven of the thirteen assigned tyrosines in BcX exhibited only two signals in a one-bond ^{13}C-HSQC spectrum (Fig. 2 and Supplemental Table S1). This results from protein fluctuations allowing rapid ring flipping to yield averaged chemical shifts for the symmetrically-related ^{1}H and ^{13}C nuclei (Snyder et al. 1975; Wüthrich and Wagner 1975). In contrast, Tyr79 and Tyr105 both yielded four signals, indicative of slow two-state flipping on the chemical shift time scale. To probe this further, we used a ^{13}C-HSQC-detected exchange experiment to measure the time-dependant intraresidue transfer of longitudinal magnetization between tyrosine $^{13}C^{\delta1}/^{13}C^{\delta2}$ or $^{13}C^{\varepsilon1}/^{13}C^{\varepsilon2}$ nuclei at 25 and 35°C (Supplemental Fig. S4) (Farrow et al. 1994). As shown in Fig. 5, the

Table 1 Summary of BcX tyrosine properties

Tyr	Hydrogen bonding[a]	Accessible surface area: ring/O^{η} ($Å^2$)[a]	$C^{\delta}/C^{\varepsilon}$ B-value ($Å^2$)[a]	HX rate constant[b]	Ring flipping rate constant[d]	pK_a^e
Y5		56/21	16.0			11.5 ± 0.1[f]
Y26	M169 O (2.9 Å)	0/0	8.8	(1.6 ± 0.01) × 10^{-4} s^{-1}		>12
Y53	D83 O^{δ} (2.6 Å) H_2O (2.9 Å)	4/1	7.5	(9.9 ± 0.1) × 10^{-4} s^{-1}		>12
Y65	H_2O (2.8 Å)	22/12	9.3			>12
Y69	E78 O^{ε} (2.6 Å) W71 $N^{\varepsilon 1}$ (3.0 Å) H_2O (2.9 Å)	7/7	8.9			>12
Y79	Q167 N^{ε} (3.1 Å) H_2O (2.7 Å)	0.1/0.1	6.9	(3.8 ± 0.4) × 10^{-6} s^{-1}	2.4 ± 0.1 s^{-1}/9.3 ± 0.5 s^{-1}	>12
Y80	E172 O^{ε} (2.7 Å) H_2O (2.8 Å)	5/5	7.9	Not assigned		
Y88		93/23	17.5			10.1 ± 0.1[g] (9.18 ± 0.34 ppm)
Y94		83/19	12.8			11.4 ± 0.1[f]
Y105	D83 O^{δ} (2.6 Å) H_2O (2.8, 2.9 Å)	0.2/0.2	7.3	0.1 s^{-1} > k_{ex} > 0.01 s^{-1}[c]	Slow/0.17 ± 0.02 s^{-1}	>12
Y108	R89 N^{η} (3.1 Å)	16/10	8.8			11.9 ± 0.1[f]
Y113		115/32	14.0			10.1 ± 0.1[g] (9.68 ± 0.47 ppm)
Y128	N159 O (2.9 Å)	17/13	8.7	Not assigned		
Y166	H_2O (2.8 Å)	19/7	11.0			11.9 ± 0.2[f]
Y174		102/34	19.3			10.3 ± 0.1[g] (9.50 ± 0.67 ppm)

[a] Based on 1XNB.pdb. Hydrogen bond distances are between O and/or N atoms. Accessible surface areas were determined with VADAR using a 1.4 Å radius sphere probe (Willard et al. 2003). B-values are average of $C^{\delta 1}/C^{\delta 2}/C^{\varepsilon 1}/C^{\varepsilon 2}$

[b] Values at pH* 4.3 and 25°C. With the exception of the unassigned Tyr80 and Tyr128, a blank entry indicates that the $^1H^{\eta}$ was not detected, presumably due to fast HX

[c] Detected in H_2O buffer but not immediately after transfer to D_2O buffer

[d] Except for Tyr80 and Tyr128, a blank entry indicates that the ring undergoes rapid flipping to yield averaged chemical shifts for the $^{13}C^{\delta}$, $^{13}C^{\varepsilon}$, $^1H^{\delta}$, and $^1H^{\varepsilon}$ nuclei. Tyr79 and Tyr105 values listed for 25/35°C

[e] pK_a values determined from the pH-dependent $^{13}C^{\zeta}$ chemical shifts. Residues with $pK_a > 12$ showed no significant shift change (i.e. <1 ppm) over the pH range examined

[f] Fit with a fixed pH-dependent chemical shift change of 9.7 ppm

[g] Fit with floating end-point chemical shifts to yield the tabulated $\Delta\delta = \delta_b - \delta_a$

presence of exchange cross peaks demonstrated that the rings of Tyr79 and Tyr105 do flip, but on the seconds timescale. Fitting of these data for the $^1H^{\varepsilon}$–$^{13}C^{\varepsilon}$ signals yielded the interconversion rate constants summarized in Table 1. The $^1H^{\delta}$–$^{13}C^{\delta}$ correlations were not analyzed due to spectral crowding. Parenthetically, we speculate that the absence of assignable signals from Tyr80 may result from conformational exchange broadening due to partially hindered ring flipping on the intermediate (msec–μsec) timescale.

Previously, the kinetics of tyrosine and phenylalanine ring flipping have been determined from one- and two-dimensional ^1H lineshape (Wagner et al. 1976; Hattori et al. 2004) or magnetization transfer measurements (Campbell et al. 1976; Nall and Zuniga 1990; Fejzo et al. 1990; Skalicky et al. 2001; Rao and Bhuyan 2007). The advantages of the ^{13}C exchange experiment presented herein include the added dispersion of a ^{13}C-HSQC spectrum, particularly when combined with amino acid selective labelling, as well as the lack of complications from interproton NOEs and the possibility to use long transfer times (relative to ^{13}C T_1) to measure slow flipping rates.

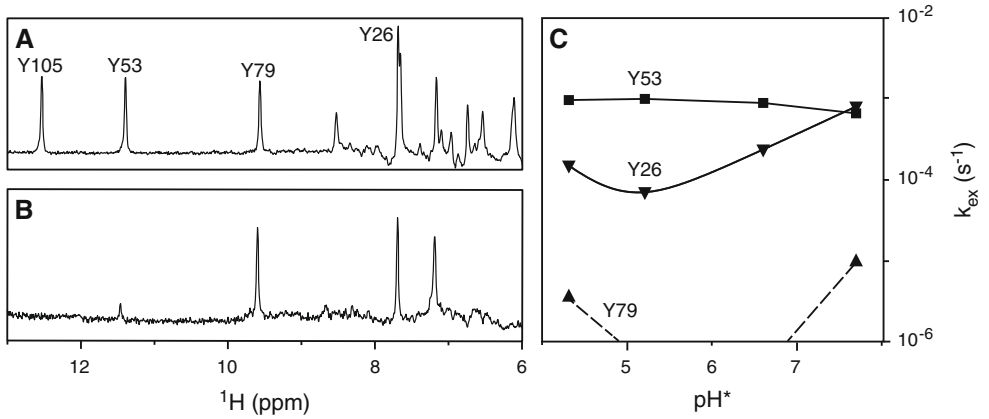

Fig. 4 The tyrosine $^1H^{\eta}$ HX rate constants were measured from $^{13}C/^{15}N$-filtered spectra of $^{13}C/^{15}N$-BcX recorded versus time after transfer to D_2O buffer. Shown are spectra of the protein in **a** H_2O and **b** after 5 min in D_2O (pH* 5.2, 25°C), along with **c** fit k_{ex} values on a logarithmic scale versus sample pH* value. Tyr79 exchanged too slowly at intermediate pH* values for reliable rate determinations over the time course of these measurements and thus $k_{ex} < 10^{-6}$ s^{-1}, as indicated by the *dashed lines*. Unassigned peaks in **a** and **b** are likely from serine or threonine hydroxyls

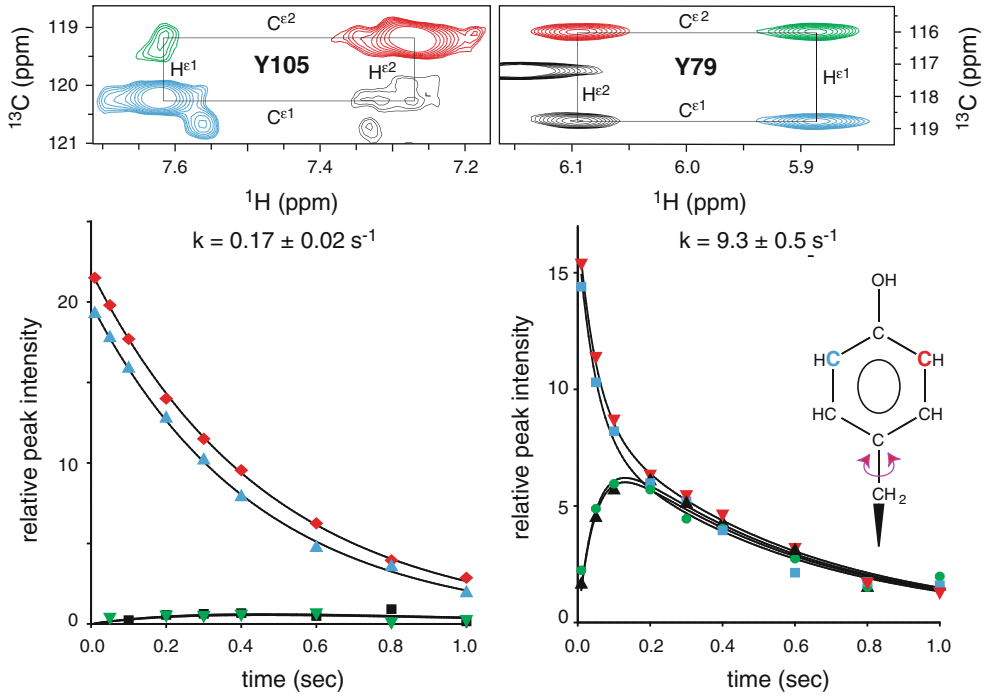

Fig. 5 The ring flipping rates of Tyr105 (*left*) and Tyr79 (*right*) were measured in ^{13}C-Tyr BcX using a longitudinal exchange experiment. Shown are selected portions of the resulting spectra recorded at 35°C with a mixing time of 400 ms for Tyr105 (*left*) and 100 ms for Tyr79 (*right*), along with the ^{13}C longitudinal decay curves of the "auto" peaks (*red*, *blue*) and build-up curves of the "exchange" peaks (*green*, *black*). The *lines* show best fits to the equations presented in the "Materials and methods" section (Tyr105: k = 0.17 ± 0.02 s^{-1}, R_1 = 2.1 ± 0.05 s^{-1} and 2.0 ± 0.04 s^{-1}; Tyr79: k = 9.3 ± 0.5 s^{-1}, R_1 = 2.2 ± 0.3 s^{-1} and 1.4 ± 0.3 s^{-1}). The auto peaks with the most downfield ^{13}C signals are assigned arbitrarily as $^{13}C^{\varepsilon 1}$–$^1H^{\varepsilon 1}$ (*blue*)

Tyrosine pK_a values

The pK_a values of the tyrosine residues in BcX were measured by monitoring their pH-dependent $^{13}C^{\zeta}$ chemical shifts (Figs. 6, 7). The $^{13}C^{\zeta}$ chemical shifts of a random coil tyrosine are ~158 and 168 ppm when its hydroxyl is neutral and deprotonated, respectively, and thus serve as a clear indicator of the ionization state of this residue (Supplemental Fig. S9) (Norton and Bradbury 1974; Oldfield et al. 1975b; Richarz and Wüthrich 1978; Boswell et al. 1983). For increased sensitivity and spectral dispersion, these shifts were obtained indirectly via two-dimensional $^{13}C^{\zeta}(^{13}C^{\varepsilon})^1H^{\varepsilon}$ (Yamazaki et al. 1993b) or $^{13}C^{\zeta}(^{13}C^{\varepsilon/\delta})^1H^{\varepsilon/\delta}$ experiments, which correlate the $^{13}C^{\zeta}$ with the $^1H^{\varepsilon}$ or $^1H^{\varepsilon/\delta}$

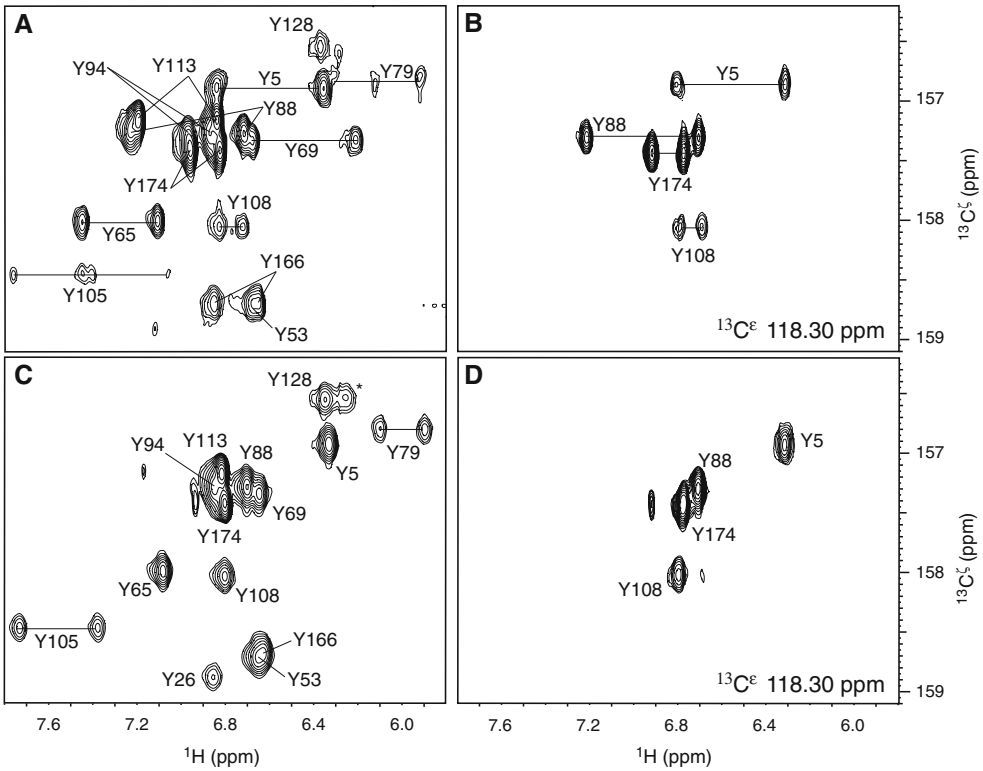

Fig. 6 pK_a titrations and tyrosine assignments were achieved using **a** $^{13}C^{\zeta}(^{13}C^{\varepsilon/\delta})^{1}H^{\varepsilon/\delta}$, **b** $^{13}C^{\zeta13}C^{\varepsilon}(^{13}C^{\delta})^{1}H^{\varepsilon/\delta}$, **c** $^{13}C^{\zeta}(^{13}C^{\varepsilon})^{1}H^{\varepsilon}$, and **d** $^{13}C^{\zeta13}C^{\varepsilon1}H^{\varepsilon}$ experiments. Panels **a** and **c** are two-dimensional spectra, whereas **b** and **d** are $\omega_1-\omega_3$ planes from three-dimensional spectra extracted at $\omega_2 = 118.30$ ppm. Tyr128 is tentatively assigned, and unassigned signal, possibly due to Tyr80, is indicated (*). See Supplemental Fig. S5–S8 for the pulse sequences

via strong one-bond couplings (Supplemental Fig. S5 and S7). The assignments of the $^{13}C^{\zeta}$ signals were facilitated by three-dimensional versions of these experiments, which also provide the $^{13}C^{\varepsilon}$ shift(s) of each aromatic ring (Fig. 6 and Supplemental Fig. S6 and S8).

Over the pH range of 6.5-10.9, three tyrosines (Tyr88, Tyr113, and Tyr174) exhibited clear $^{13}C^{\zeta}$-monitored titrations corresponding to fit pK_a values of 10.1–10.3 (Fig. 7; Table 1). These relatively unperturbed values are similar to that of 9.8 reported for a tyrosine in a random coil polypeptide (Thurlkill et al. 2006; Grimsley et al. 2009). As expected, the three are the most solvent exposed tyrosines in BcX and their hydroxyls are not involved in intramolecular hydrogen bonding. Four additional partially buried tyrosines showed small pH-dependent $^{13}C^{\zeta}$ chemical shift changes with increasing sample pH, yielding estimated pK_a values of 11.4–11.9. In contrast, the remaining seven tyrosines with assigned signals did not titrated significantly. Given that their $^{13}C^{\zeta}$ shifts are diagnostic of the neutral state (Fig. 7), it is safe to conclude that these residues have pK_a values >12. As also expected, this latter group includes the well buried Tyr26, Tyr26, Tyr79, and Tyr105. The above conclusions are supported by a parallel analysis of the pH-dependent $^{1}H^{\delta/\varepsilon}$ chemical shifts of these residues (Supplemental Fig. S10). It should be mentioned that all tyrosine hydroxyls in BcX are exchangeable with the solvent, and thus the lack of detectable pH-titrations is unlikely a kinetic issue. Also, BcX remains folded under alkaline conditions since its tyrosines still give well resolved, native state ^{13}C- and ^{1}H-NMR signals at even pH 10.9.

Discussion

Detection of tyrosine $^{1}H^{\eta}$ by NMR spectroscopy

Currently, chemical shifts for only 145 tyrosine $^{1}H^{\eta}$ nuclei from diamagnetic proteins have been deposited in the BioMagResBank (Ulrich et al. 2008). Most of these $^{1}H^{\eta}$ signals appear to have been identified and assigned based on interproton NOEs. This low number, which corresponds to ~1% of the reported tyrosine amide shifts, certainly results in large part from the facile HX of sidechain hydroxyl groups under conditions typically used for protein NMR spectroscopy. However, the assigned $^{1}H^{\eta}$ signals range from 5.99 to 13.75 ppm and cluster near an average value of 9.31 ppm with a standard deviation 1.37 ppm (Ulrich et al. 2008). Thus, it is likely that many HX-protected tyrosine hydroxyls are undetected simply because their signals are hidden under those of the amide and aromatic protons in 1D ^{1}H-NMR spectra, and because they are not observable in "work horse" one-bond ^{15}N- or ^{13}C-HSQC spectra. Weakly protected $^{1}H^{\eta}$ nuclei may also be unnoticed when employing pre-saturation, rather than selective pulses, for water suppression.

Using BcX as a model system, we have found that signals from tyrosine $^{1}H^{\eta}$ nuclei protected from rapid HX can be readily detected in a simple $^{13}C/^{15}N$-filtered ^{1}H-NMR spectrum measured with a uniformly $^{13}C/^{15}N$-labeled protein sample. Residue specific assignments can then be obtained from a long range ^{13}C-HSQC, best recorded with

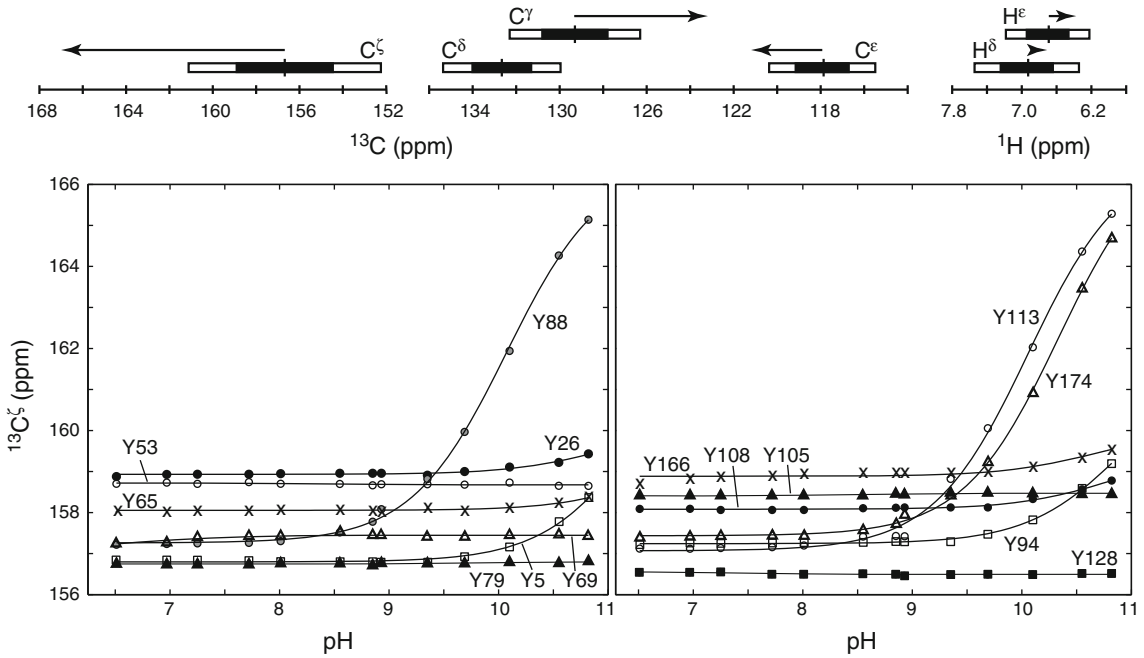

Fig. 7 The pH-dependent $^{13}C^{\zeta}$ chemical shifts of the tyrosine residues in BcX (35°C) measured from the $^{13}C^{\zeta}(^{13}C^{\varepsilon/\delta})^{1}H^{\varepsilon/\delta}$ experiment (*lower panels*). The *lines* represent the best fits to a single pK_a value with a fixed pH dependent chemical shift change ($\delta_b-\delta_a$) of 9.7 ppm, except for Tyr88, Tyr113, and Tyr174 for which floating end-points were allowed. The fit pK_a values and chemical shift changes are summarized in Table 1. Also shown in the *upper panel* are the mean ^{13}C and ^{1}H chemical shifts of tyrosine ring nuclei in diamagnetic proteins, as reported in the BioMagResBank (Ulrich et al. 2008), with solid and open boxes indicating a range of one and two standard deviations, respectively. The *arrows* indicate the directions and magnitudes of the chemical shift changes expected upon deprotonation (Norton and Bradbury 1974; Richarz and Wüthrich 1978; Bundi and Wüthrich 1979). See also Supplemental Fig. S9 and S10

a ^{13}C-tyrosine selectively labeled sample. Indeed, a 1D difference spin echo version of this approach, which exploits the weak $^{3}J_{CH}$ coupling between the $^{1}H^{\eta}$ and $^{13}C^{\varepsilon}$ nuclei, was first used to identify a tyrosine hydroxyl buried at the interface between the DNA-binding Ets-1 ETS domain and a consensus oligonucleotide (Werner et al. 1997). Alternatively, a $^{13}C/^{15}N$-filtered/edited NOESY-HSQC spectrum recorded with a protein highly enriched in ^{13}C and ^{15}N can also be exploited to detect and assign these signals, albeit with the inherent ambiguity of a through space interaction. Although this latter experiment is typically used to detect intermolecular NOEs within a complex of isotopically labeled and unlabeled species (Ikura and Bax 1992; Zwahlen et al. 1997), intramolecular NOEs involving oxygen- or sulfur-bonded protons will also be observed for an isolated $^{13}C/^{15}N$-protein.

Structural characterization of Tyr79 and Tyr105

The observation of both slow ring flipping and slow HX for Tyr79 and Tyr105 presented an interesting opportunity to characterize the structural features of these two tyrosine residues (Fig. 8). By way of background, recall that phenol is a planar molecule with its O^{η} sp^2-hydridized (Carey and Giuliano 2011). Furthermore, neutron and very high resolution X-ray crystallographic studies confirm that tyrosines in proteins preferentially adopt planar rotameric states with the χ_3 dihedral angle ($C^{\varepsilon 1}$–C^{ζ}–O^{η}–H^{η}) near 0° or 180° (Kossiakoff et al. 1990; Ho and Agard 2008). Inspection of the long-range ^{13}C-HSQC spectrum of BcX revealed crosspeaks between the $^{1}H^{\eta}$ of Tyr79 and Tyr105 and only one of their two non-degenerate $^{13}C^{\varepsilon}$ nuclei (Figs. 2, 8). Based on the Karplus relationship for a $^{3}J_{CH}$ coupling (Karplus 1959), the detected $^{13}C^{\varepsilon}$ must be oriented in a "trans" conformation relative to the $^{1}H^{\eta}$. This conclusion is supported by the observation of a strong intra-residue NOE between the $^{1}H^{\eta}$ and the adjacent $^{1}H^{\varepsilon}$ directly bonded to the "cis" $^{13}C^{\varepsilon}$ in each ring. Together, these data indicate that the hydroxyl groups of Tyr79 and Tyr105 are well ordered with respect to their aromatic rings and do not undergo facile rotation about the C^{ζ}–O^{η} bond.

Having defined the positions of the $^{1}H^{\eta}$ relative to the rings of Tyr79 and Tyr105, we then used inter-residue NOEs to orient these rings in the X-ray crystallographic structure of BcX. The aromatic ring of Tyr79 is surrounded by hydrophobic sidechains, and its O^{η} is within hydrogen bonding distance of a buried water (2.7 Å) and the amide $N^{\varepsilon 2}$ of Gln167 (3.1 Å) (Fig. 8g; Table 1). Given the NMR-defined position of its $^{1}H^{\eta}$, Tyr79 must donate a hydrogen bond to the water and accept one from the glutamine. This

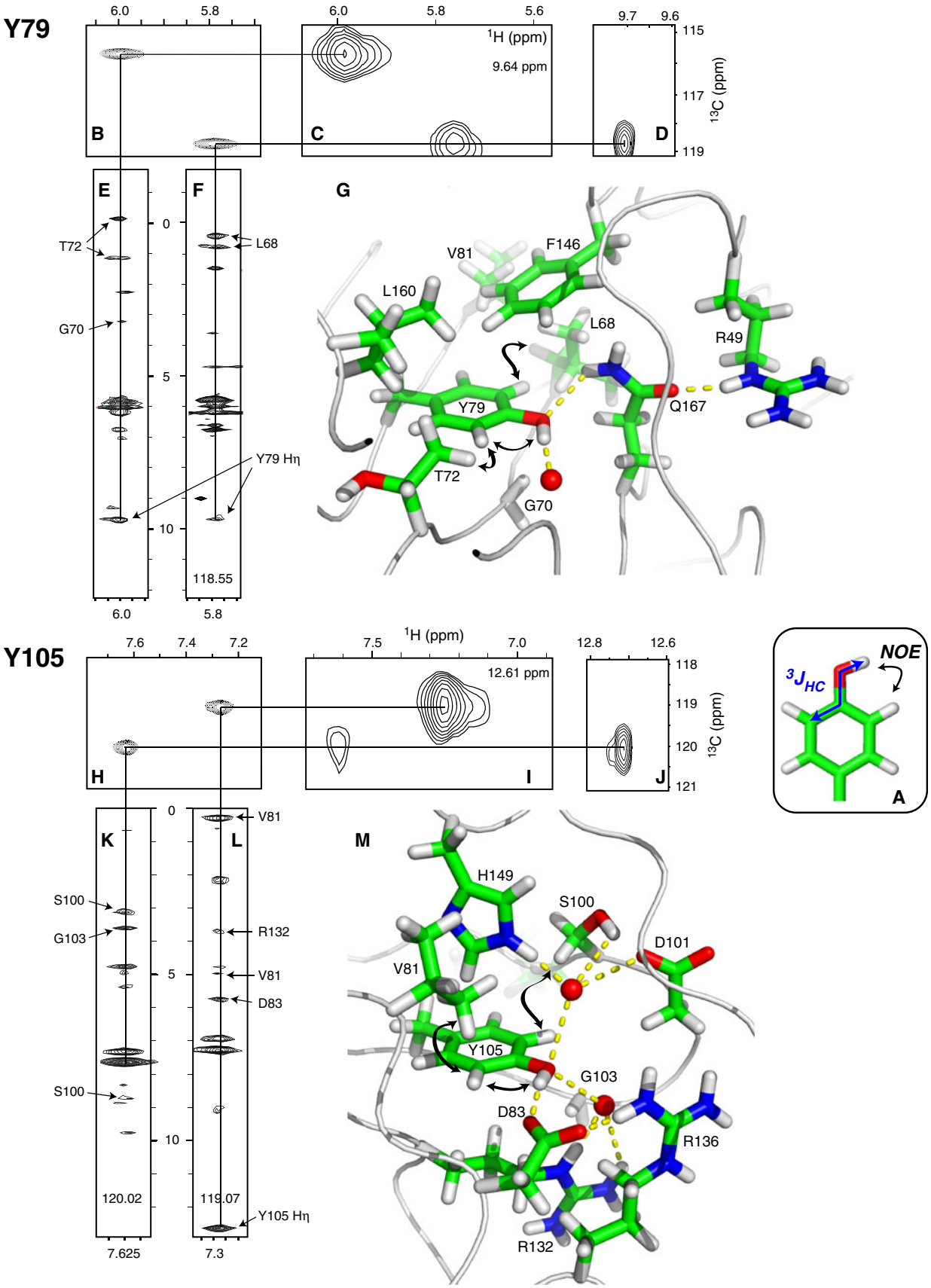
Y79
B
C
D
E
F
G
^{1}H (ppm)
9.64 ppm
^{13}C (ppm)
T72
G70
L68
Y79 Hη
118.55
V81
F146
L160
L68
R49
Q167
Y79
T72
G70
Y105
H
I
J
K
L
M
12.61 ppm
S100
G103
R132
V81
D83
120.02
119.07
Y105 Hη
H149
D101
R136
NOE
$^3J_{HC}$
A

◀ **Fig. 8** **a** Due to slow ring flipping and slow rotation about the C^{ζ}–O^{η} bond, the hydroxyl H^{η} of Tyr79 and Tyr105 can be positioned within BcX using interproton NOE and $^{3}J_{CH}$ coupling information. **b**, **h** Portions of one-bond ^{13}C-HSQC spectra with crosspeaks from the non-degenerate $^{1}H^{\varepsilon}$–$^{13}C^{\varepsilon}$ of the two tyrosine. **c**, **i** $\omega_2-\omega_3$ planes of a ^{13}C/^{15}N-filtered/edited NOESY-HSQC spectrum of ^{13}C/^{15}N-BcX ($\tau_{mix} = 0.15$ ms; 35°C) taken at the indicated $^{1}H^{\eta}$ chemical shifts of the two tyrosines. This experiment detects only NOEs from the unlabelled $^{1}H^{\eta}$ to nearby labelled protons (Zwahlen et al. 1997). In each panel, the strong crosspeak arises from the adjacent cis-oriented $^{1}H^{\eta}$ and $^{1}H^{\varepsilon}$ (~2.2 Å separation), whereas the weaker crosspeak is due to a longer range NOEs to the distal $^{1}H^{\varepsilon}$ (~3.6 Å) and/or some flipping about the C^{ζ}–O^{η} bond. **d**, **j** In contrast, the distal $^{13}C^{\varepsilon}$ is trans to the $^{1}H^{\eta}$ and thus detected in a long range ^{13}C-HSQC spectrum. **e**, **f**, **k**, **l** Finally, the aromatic rings are positioned via inter-residue NOEs, shown in $\omega_1-\omega_3$ planes of a ^{13}C,^{15}N-edited NOESY-HSQC spectrum of ^{13}C/^{15}N BcX taken at the indicated $^{13}C^{\varepsilon}$ shifts of the two tyrosines ($\tau_{mix} = 0.1$ ms; 35°C). This experiment yields NOEs from both labelled and unlabelled protons to the labelled $^{1}H^{\varepsilon}$. Selected crosspeaks are assigned. **g**, **m** The local environments of Tyr79 and Tyr105 in the crystal structure of BcX (1XNB.pdb; oxygen *red*; nitrogen *blue*; carbon *green*; hydrogen *grey*). Hydrogens were added to the protein coordinate file with the program Reduce (Word et al. 1999) and the tyrosines manually adjusted to planarity. The charge and tautomeric states of Aps83, Asp101, and His149 have been verified experimentally, whereas arginines are assumed to be fully protonated under neutral pH conditions. Bound water molecules are shown as *red balls*. Potential hydrogen bonds are indicated with *yellow dashes*. Examples of proton pairs yielding key NOEs used to orient the tyrosine rings are identified with *black arrows*

is consistent with the $O^{\varepsilon 1}$ of Gln167 accepting a hydrogen bond from Arg49 and argues against flipping the amide group of this residue to reverse the donor/acceptor behaviour of Tyr79. Intriguingly, these data indicate that Tyr79 shows significant protection against HX despite donating a hydrogen bond to a buried water. A similar situation has been documented for the protected $N^{\varepsilon 2}H$ of neutral His149 in BcX (Connelly and McIntosh 1998).

Tyr105 participates in a fascinating set of polar interactions within the interior of BcX (Fig. 8m; Table 1). In light of our current NMR results, this tyrosine donates a strong hydrogen bond to the $O^{\delta 1}$ of Asp83 (2.6 Å). This may account for its highly downfield shifted $^{1}H^{\eta}$ signal at 12.53 ppm. Previous studies have shown that Asp83 has a $pK_a < 2$ and thus is negatively-charge within the folded structure of BcX, forming a buried salt bridge with Arg136 (Joshi et al. 1997; McIntosh et al. 2011). Parenthetically, Asp83 $O^{\delta 2}$ is also positioned to accept a hydrogen bond from the detectable $^{1}H^{\eta}$ of Tyr53. Having defined the relative location of Tyr105 $^{1}H^{\eta}$ by NMR methods, we conclude that two crystallographically-identified buried waters must be donating hydrogen bonds to the O^{η} of this aromatic sidechain (2.8 and 2.9 Å). One of these waters also accepts hydrogen bonds from Arg132 and the other is tightly positioned by negatively-charged Asp101 [$pK_a < 2$ (Joshi et al. 1997)], the above mentioned neutral His149 [$pK_a < 2.3$ (Plesniak et al. 1996a)], and Ser100. Surprisingly, despite these extensive interactions and its slow rate of ring flipping, Tyr105 exhibits less protection from HX than does Tyr79.

Tyrosine dynamics and hydroxyl HX

Complementary insights into the dynamic properties of the BcX tyrosines were obtained using NMR spectroscopy to measure their ring flipping and HX kinetics. In particular, the four residues with detectable $^{1}H^{\eta}$ signals had $k_{ex} < 0.1\ s^{-1}$ over the pH range examined and hence estimated HX protection factors of $\sim 10^4$–10^8. As expected, each of these sidechain hydroxyls is sequestered from bulk solvent due to burial and hydrogen bonding within the core of BcX. Given that $^{1}H^{\eta}$ resonances from the remaining tyrosines were not detected in spectra recorded at pH 6.5 in H_2O buffer, these residues likely undergo rapid HX with k_{ex} greater than 10–100 s^{-1} and thus have protection factors less than 1,000–100 under these conditions (Liepinsh et al. 1992; Liepinsh and Otting 1996). The first of these two order-of-magnitude limits reflect the fact that if $k_{ex} > {}^{3}J_{CH}$ ~5 Hz, then loss of polarization transfer will preclude detection of the $^{1}H^{\eta}$ signal in a long range ^{13}C-HSQC spectrum (Henry and Sykes 1990). The second assumes that line broadening of more than about 30 Hz due to exchange (Δlinewidth $= k_{ex}/\pi$ at half-height) will preclude detection in a 1D ^{1}H-NMR spectrum, particularly if requiring an echo delay for ^{13}C/^{15}N-filtering. More accurate rates or rate limits could be obtained by the elegant approach of Kainosho and co-workers, which relies upon the interplay of exchange kinetics and an ~0.13 ppm deuterium isotope shift experienced by the phenolic $^{13}C^{\zeta}$ in D_2O versus H_2O solutions (Takeda et al. 2009). Of course, this also assumes that none of these residues has a protected $^{1}H^{\eta}$ with a chemical shift upfield of ~7 ppm, as such a signal might be obscured by the various multiple-bond correlations between non-labile ^{1}H and ^{13}C nuclei in the spectrum of Fig. 1c. Consistent with this conclusion, each of these apparently rapidly exchanging tyrosines has a hydroxyl O^{η} that is at least partially solvent exposed in the crystal structure of BcX (Table 1).

Classically, HX kinetics are interpreted in terms of local or global conformational fluctuations between a closed and an open state ($K_{eq} = k_{open}/k_{close}$). Exchange occurs from the unprotected open state with the pseudo-first order rate constant (k_{pred}) predicted for the mainchain or sidechain moiety in a reference random coil polypeptide under similar experimental conditions (Hvidt and Nielsen 1966; Englander and Kallenbach 1983). In the case of Tyr53, exchange appeared to approach the pH-independent EX1 limit. If so, the measured $k_{ex} \sim 10^{-3}\ s^{-1}$ likely corresponds to the rate constant k_{open} for conformational fluctuations leading to an exchange competent open state. This also implies that the closing rate constant k_{close} for those

fluctuations is slower than the $k_{pred} \sim 10^3\ s^{-1}$ estimated for an unprotected tyrosine at pH ~4.3 such that exchange occurs with every opening event (Liepinsh et al. 1992; Liepinsh and Otting 1996). Accordingly, $K_{eq} > 10^{-6}$ for the conformational fluctuations leading to HX of the Tyr53 hydroxyl. As mentioned above in reference to the crystal structure of BcX, this protected tyrosine most likely donates a hydrogen bond to the negatively-charged sidechain of buried Asp83 [$pK_a < 2$ (Joshi et al. 1997)] and accepts one from a bound water (Table 1).

In contrast to Tyr53, both Tyr26 and Tyr79 exhibited pH-dependent HX indicative of a pre-equilibrium or EX2 mechanism. In this case, $k_{close} > k_{pred}$ and $k_{ex} = K_{eq}\ k_{pred}$. Thus, the protection factor k_{pred}/k_{ex} is the inverse of the equilibrium constant for the conformational fluctuations from the closed to the open state. Converting to a free energy scale, the protection factors of 10^7 and 10^8 estimated for Tyr26 and Tyr79 correspond to $\Delta G°_{HX}$ values of 9.6 and 10.9 kcal/mol, respectively. Although substantial, the free energy change for global unfolding of BcX could still be larger than these values, as suggested by its highly ordered main chain (Connelly et al. 2000) and its irreversible denaturation at a midpoint temperature $T_m \sim 60°C$ (Davoodi et al. 1995) and $[urea]_m \sim 5.5$ M (pH 5.5 and 20°C; unpublished results). In the crystal structure of BcX, Tyr26 appears to donate a hydrogen bond to the carbonyl oxygen of Met169, whereas NMR data demonstrates that Tyr79 accepts a hydrogen bond from the sidechain nitrogen of Gln167 and donates one to a bound water (Fig. 8g). Although readily detectable, the $^1H^{\eta}$ of Tyr105 exchanged with water on a timescale too fast for measurement after transfer to D_2O buffer, yet too slow for analysis by magnetization transfer approaches. Thus, insights into the kinetic mechanism of Tyr105 HX were not obtained. As shown in Fig. 8m, this latter residue also donates a hydrogen bond to the carboxylate of buried Asp83 and accepts hydrogen bonds from two bound waters.

Tyrosine dynamics and ring flipping

The observation that the stereochemically equivalent nuclei of aromatic rings located within the anisotropic environment of a protein typically show averaged chemical shifts provided some of the earliest and clearest evidence for the dynamic nature of these biopolymers (Snyder et al. 1975; Wüthrich and Wagner 1975). Indeed, based on an analysis of assignments reported in the BioMagResBank, Skalicky et al. (Skalicky et al. 2001) estimated that >95% of all tyrosine and phenylalanine rings in proteins undergo fast flipping ($>10^3\ s^{-1}$) on the chemical shift time scale at ambient temperatures, thereby yielding such averaged signals. Conversely, distinct signals from $\delta1/\delta2$ to $\varepsilon1/\varepsilon2$ nuclei (indicative of hindered ring flipping on this timescale) have been detected in a surprisingly limited number of examples. This behaviour presumably results from slower conformational fluctuations yielding transient cavities in which an aromatic sidechain can undergo a rapid two-site jump between symmetrically equivalent positions differing by only a 180° rotation about the C^{β}–C^{γ} bond. Through temperature- and pressure-dependent ^1H lineshape or magnetization transfer measurements, the rate constants and activation $\Delta H^{\ddagger}$, $\Delta S^{\ddagger}$, and $\Delta V^{\ddagger}$ parameters for these fluctuations have been characterized in a few proteins (Wagner et al. 1976; Wagner 1980; Nall and Zuniga 1990; Skalicky et al. 2001; Hattori et al. 2004; Rao and Bhuyan 2007).

Consistent with these general observations, only two of the fifteen tyrosines in BcX showed four distinct, rather than two averaged, signals from ring ^{13}C–^1H pairs diagnostic of slow ring flipping. Using a ^{13}C longitudinal exchange experiment, flipping rate constants of ~10 and ~0.2 s^{-1} were measured for Tyr79 and Tyr105, respectively. The remaining assigned tyrosines must rotate at least 100-fold faster in order to yield averaged NMR signals. Although it is expected that surface tyrosines such as Tyr88, Tyr113, and Tyr174 show relatively unimpeded motions, several of these fast flipping residues are extensively buried. Skalicky et al. (Skalicky et al. 2001) also reported that solvent accessibility alone is not a key parameter for identifying slowly rotating rings. This prompts the question as to why only Tyr79 and Tyr105 flip slowly. Interestingly, in the X-ray crystallographic structure of BcX (1XNB.pdb), these two residues have the lowest average $C^{\delta/\varepsilon}$ thermal factors (B values) of all tyrosines, indicating that they are well ordered within the protein core. Although a similar trend was reported for the slowest flipping tyrosines in yeast iso-2-cytochrome c (Nall and Zuniga 1990), other faster flipping buried residues have only marginally higher average B values. It is also noteworthy that all four tyrosines in BcX with detectable $^1H^{\eta}$ signals exhibited faster ring flipping than hydroxyl HX. For example, the flipping rate constant of Tyr53 must be $>10^3\ s^{-1}$ to yield averaged NMR signals, whereas the opening rate constant, $k_{open} \sim 10^{-3}\ s^{-1}$, for its apparent EX1-regmine HX is at least 10^6-fold slower. Furthermore, Tyr105 showed more hindered rotation, yet faster HX, than Tyr79. Thus, conformational fluctuations allowing a two-site jump about the C^{β}–C^{γ}–C^{ζ}–O^{η} axis of an aromatic sidechain are not correlated with those disrupting hydrogen bonding interactions with its hydroxyl OH, as required for HX with water. A similar lack of correlation between ring flipping and protein stability/amide HX was also reported for a series of BPTI homologs (Wagner and Wüthrich 1978).

Collectively, the current studies of tyrosine ring flipping and hydroxyl HX, along with previous amide ^{15}N relaxation measurements (Connelly et al. 2000), highlight the complex dynamics exhibited by the backbone and

sidechain residues of BcX. These NMR data should also serve as a benchmark for the development of theoretical approaches to better describe the amplitudes and timescales of the conformational fluctuations of a protein in its native state ensemble.

Tyrosine pK_a measurements

The pK_a value of a tyrosine in a random coil polypeptide is ~10. (Thurlkill et al. 2006; Grimsley et al. 2009). Thus, within the context of a folded protein under physiological conditions, the vast majority of these sidechains are expected to exist in the neutral state. Of course, functionally critical tyrosines, such as those serving as a catalytic nucleophile or general acid/base, should be charged in their active form and thus will have significantly perturbed pK_a values (Harris and Turner 2002). For example, the general base Tyr149 in UDP-galactose 4-epimerase is reported to have a remarkably low pK_a value of 6.09, as determined by kinetic and uv absorbance analyses (Liu et al. 1997). However, in the limited number of proteins for which site specific measurements have been made, the pK_a values of tyrosine sidechains are almost always >10. Consistent with this observation, three solvent exposed tyrosines in BcX titrated with pK_a values ranging from 10.1 to 10.3, four showed partial titrations with fit pK_a values of 11.4–11.9, and the remaining most buried residues were neutral under all conditions examined and thus must have pK_a values >12. The unfavourable ionization of the latter tyrosines likely reflects the energetic penalty of burying a negative charge within the low dielectric core of the protein, along with the potential changes in hydrogen bonding interactions and local or global electrostatic repulsion (i.e., the theoretical pI of BcX is 9.05).

Initially, NMR spectroscopists investigated tyrosine pK_a values by directly monitoring the pH-dependent $^{13}C^{\zeta}$ chemical shifts of these residues (Oldfield et al. 1975a; Grissom and Markley 1989). However, subsequent studies tended to focus on tyrosine $^{1}H^{\varepsilon/\delta}$ shifts, measured by one- or two-dimensional homonuclear ^{1}H-NMR methods (Karplus et al. 1973; Wagner and Wüthrich 1975; Chinami and Shingu 1989; Khare et al. 1997), and $^{13}C^{\varepsilon/\delta}$ shifts recorded indirectly by one-bond ^{13}C-HSQC experiments (Sun et al. 2004). In this study, we have exploited two-dimensional $^{13}C^{\zeta}(^{13}C^{\varepsilon})^{1}H^{\varepsilon}$ (Yamazaki et al. 1993b) or $^{13}C^{\zeta}(^{13}C^{\varepsilon/\delta})^{1}H^{\varepsilon/\delta}$ experiments to measure $^{13}C^{\zeta}$ shifts indirectly with the added dispersion and sensitivity afforded by direct detection of the $^{1}H^{\varepsilon/\delta}$ nuclei within the same ring. The advantages of using $^{13}C^{\zeta}$ chemical shifts to monitor tyrosine pH-titrations are threefold. First, of all possible ring ^{1}H or ^{13}C nuclei, the $^{13}C^{\zeta}$ exhibits the largest chemical shift change (~10 ppm) upon ionization and thus provides the highest dynamic range for pK_a measurements. Second, as shown in Fig. 7c, this chemical shift change is substantially larger than the range of chemical shift perturbations expected from the specific environment of a tyrosine with a folded protein. A $^{13}C^{\zeta}$-measured titration curve can therefore, be attributed with high confidence to the actual ionization equilibrium of a given tyrosine. In contrast, for the ring C–H groups, the chemical shift differences between the neutral and negatively-charged forms of a tyrosine are comparable to ($^{13}C^{\varepsilon}$) or less than ($^{1}H^{\delta}$, $^{1}H^{\varepsilon}$) those inducible by protein structure (and $^{13}C^{\delta}$ is insensitive to ionization). Thus, the origin of any pH-dependent chemical shift changes shown by these nuclei may be ambiguous. This is clearly illustrated by the degenerate $^{1}H^{\delta}$ of Tyr69, which undergo a substantial −0.31 ppm change following a pK_a value of 6.9 (Supplemental Fig. S10). Given that the $^{13}C^{\zeta}$ chemical shift of this active site tyrosine remained constant over all pH conditions examined, this apparent titration is certainly due to the ionization of the adjacent catalytic general acid Glu172, rather than Tyr69 itself. Third, in the absence of any measurable titration, the pK_a value of an ionizable residue could be less than or greater than the lowest or highest sample pH value examined, respectively. Given that the $^{13}C^{\zeta}$ chemical shifts of a neutral and charged tyrosine are ~158 and 168 ppm, it is safe to say that all of these residues in BcX are protonated under neutral conditions (Fig. 7). In contrast, such a conclusion cannot be drawn unambiguously from $^{13}C^{\delta/\varepsilon}$ or $^{1}H^{\delta/\varepsilon}$ shifts alone. Thus, alternative approaches for determining the protonation state of an ionizable sidechain, such as direct observation of the titratable proton, as well as the measurement of deuterium isotope shifts (Ladner et al. 1975; Yamazaki et al. 1994; Joshi et al. 1997; Takeda et al. 2009) or J-coupling patterns (Pelton et al. 1993; McIntosh et al. 2006; Iwahara et al. 2008), would be required. Although not investigated in this study, the $^{13}C^{\gamma}$ of a tyrosine also shows a substantial chemical shift change (~−6.5 ppm) upon deprotonation, and thus the above advantages should also apply for determining pK_a values by monitoring this nucleus. Fortunately, pulse sequences for measuring tyrosine $^{13}C^{\gamma}$ chemical shifts via their sidechain $^{1}H^{\beta}$, $^{1}H^{\delta}$, and/or $^{1}H^{\varepsilon}$ nuclei have also been published (Prompers et al. 1998).

Summary

In closing, we have used a combination of established and new NMR spectroscopic methods to characterize the structural (J-coupling, NOE), dynamic (HX, ring flipping), and thermodynamic (pK_a values) properties of the tyrosine residues in BcX. In addition to providing specific insights into the roles played by these aromatic sidechains in this model glycoside hydrolase, we hope this work will stimulate further studies of these functionally and structurally

important residues in other interesting proteins and protein complexes.

Acknowledgments We thank Lewis Kay for continued advice and NMR pulse sequences, as well as Frans Mulder and Jens Nielsen for helpful discussions. This research was funded by the Natural Sciences and Engineering Research Council of Canada (NSERC) to LPM. SJB acknowledges a UBC Aboriginal Graduate Fellowship. Instrument support was provided by the Canadian Institutes for Health Research (CIHR), the Canadian Foundation for Innovation (CFI), the British Columbia Knowledge Development Fund (BCKDF), the UBC Blusson Fund, and the Michael Smith Foundation for Health Research (MSFHR).

References

Barry BA, Einarsdottir O (2005) Insights into the structure and function of redox-active tyrosines from model compounds. J Phys Chem B 109:6972–6981

Bax A, Summers MF (1986) Proton and carbon-13 assignments from sensitivity-enhanced detection of heteronuclear multiple-bond connectivity by 2D multiple quantum NMR. J Am Chem Soc 108:2093–2094

Boswell AP, Moore GR, Williams RJP, Harris DE, Wallace CJA, Bocieck S, Welti D (1983) Ionization of tyrosine and lysine residues in native and modified horse cytochrome-c. Biochem J 213:679–686

Bundi A, Wüthrich K (1979) ^{1}H-NMR parameters of the common amino-acid residues measured in aqueous-solutions of the linear tetrapeptides H-Gly-Gly-X-L-Ala-OH. Biopolymers 18:285–297

Campbell ID, Dobson CM, Moore GR, Perkins SJ, Williams RJP (1976) Temperature-dependent molecular-motion of a tyrosine residue of ferrocytochrome-C. FEBS Lett 70:96–100

Cantarel BL, Coutinho PM, Rancurel C, Bernard T, Lombard V, Henrissat B (2009) The carbohydrate-active EnZymes database (CAZy): an expert resource for glycogenomics. Nucl Acids Res 37:D233–D238

Carey FA, Giuliano RM (2011) Organic chemistry, 8th edn. McGraw-Hill, NY

Chinami M, Shingu M (1989) Hydrogen-1 nuclear magnetic resonance studies of staphylococcal nuclease variant H124L: pH-dependence of histidines and tyrosines. Arch Biochem Biophys 270:126–136

Connelly GP, McIntosh LP (1998) Characterization of a buried neutral histidine in *Bacillus circulans* xylanase: internal dynamics and interaction with a bound water molecule. Biochemistry 37:1810–1818

Connelly GP, Withers SG, McIntosh LP (2000) Analysis of the dynamic properties of *Bacillus circulans* xylanase upon formation of a covalent glycosyl-enzyme intermediate. Prot Sci 9:512–524

Creighton TE (2010) The biophysical chemistry of nuclei acids and proteins. Helvetian Press, NY

Davoodi J, Wakarchuk WW, Campbell RL, Carey PR, Surewicz WK (1995) Abnormally high pKa of an active-site glutamic acid residue in *Bacillus circulans* xylanase. The role of electrostatic interactions. Eur J Biochem 232:839–843

Delaglio F, Grzesiek S, Vuister GW, Zhu G, Pfeifer J, Bax A (1995) NMRpipe—a multidimensional spectral processing system based on UNIX pipes. J Biomol NMR 6:277–293

DeLano WL (2004) Use of PYMOL as a communications tool for molecular science. Abstr Pap Am Chem Soc 228:U313–U314

Englander SW, Kallenbach NR (1983) Hydrogen exchange and structural dynamics of proteins and nucleic acids. Q Rev Biophys 16:521–655

Farrow NA, Zhang O, Forman-Kay JD, Kay LE (1994) A heteronuclear correlation experiment for simultaneous determination of ^{15}N longitudinal decay and chemical exchange rates of systems in slow equilibrium. J Biomol NMR 4:727–734

Fejzo J, Westler WM, Macura S, Markley JL (1990) Elimination of cross-relaxation effects from 2-dimensional chemical-exchange spectra of macromolecules. J Am Chem Soc 112:2574–2577

Goddard TD, Kneeler DG (1999) Sparky 3. University of California, San Francisco

Grimsley GR, Scholtz JM, Pace CN (2009) A summary of the measured pK values of the ionizable groups in folded proteins. Prot Sci 18:247–251

Grissom CB, Markley JL (1989) Staphylococcal nuclease active-site amino acids: pH-dependence of tyrosines and arginines by ^{13}C NMR and correlation with kinetic studies. Biochemistry 28: 2116–2124

Harris TK, Turner GJ (2002) Structural basis of perturbed pK(a) values of catalytic groups in enzyme active sites. IUBMB Life 53:85–98

Hattori M, Li H, Yamada H, Akasaka K, Hengstenberg W, Gronwald W, Kalbitzer HR (2004) Infrequent cavity-forming fluctuations in HPr from *Staphylococcus carnosus* revealed by pressure- and temperature-dependent tyrosine ring flips. Prot Sci 13:3104–3114

Henry GD, Sykes BD (1990) Hydrogen exchange kinetics in a membrane protein determined by ^{15}N NMR spectroscopy: use of the INEPT experiment to follow individual amides in detergent-solubilized M13 coat protein. Biochemistry 29:6303–6313

Ho BK, Agard DA (2008) Identification of new, well-populated amino-acid sidechain rotamers involving hydroxyl-hydrogen atoms and sulfhydryl-hydrogen atoms. BMC Struct Biol 8:41

Holliday GL, Mitchell JBO, Thornton JM (2009) Understanding the functional roles of amino acid residues in enzyme catalysis. J Mol Biol 390:560–577

Hvidt A, Nielsen SO (1966) Hydrogen exchange in proteins. Adv Prot Chem 21:287–386

Hwang TL, Mori S, Shaka AJ, van Zijl PCM (1997) Application of phase-modulated CLEAN chemical EXchange spectroscopy (CLEANEX-PM) to detect water-protein proton exchange and intermolecular NOEs. J Am Chem Soc 119:6203–6204

Ikura M, Bax A (1992) Isotope-filtered 2D NMR of a protein peptide complex: study of a skeletal-muscle myosin light chain kinase fragment bound to calmodulin. J Am Chem Soc 114:2433–2440

Iwahara J, Takayama Y, Castaneda CA, Chimenti M, Garcia-Moreno B (2008) Direct evidence for deprotonation of a lysine side chain buried in the hydrophobic core of a protein. J Am Chem Soc 130:6714–6715

Joshi MD, Hedberg A, McIntosh LP (1997) Complete measurement of the pKa values of the carboxyl and imidazole groups in *Bacillus circulans* xylanase. Prot Sci 6:2667–2670

Joshi MD, Sidhu G, Nielsen JE, Brayer GD, Withers SG, McIntosh LP (2001) Dissecting the electrostatic interactions and pH-dependent activity of a family 11 glycosidase. Biochemistry 40:10115–10139

Karplus M (1959) Contact electron-spin coupling of nuclear magnetic moments. J Chem Phys 30:11–15

Karplus S, Snyder GH, Sykes BD (1973) A nuclear magnetic resonance study of bovine pancreatic trypsin-inhibitor. Tyrosine titrations and backbone NH groups. Biochemistry 12:1323–1329

Khare D, Alexander P, Antosiewicz J, Bryan P, Gilson M, Orban J (1997) pK(a) measurements from nuclear magnetic resonance for the B1 and B2 immunoglobulin G-binding domains of protein G: Comparison with calculated values for nuclear magnetic resonance and x-ray structures. Biochemistry 36:3580–3589

Kim HW, Perez JA, Ferguson SJ, Campbell ID (1990) The specific incorporation of labelled aromatic amino acids into proteins through growth of bacteria in the presence of glyphosate. Application to fluorotryptophan labelling to the H(+)-ATPase of *Escherichia coli* and NMR studies. FEBS Lett 272:34–36

Kossiakoff AA, Shpungin J, Sintchak MD (1990) Hydroxyl hydrogen conformations in trypsin determined by the neutron-diffraction solvent difference map method: relative importance of steric and electrostatic factors in defining hydrogen-bonding geometries. Proc Natl Acad Sci 87:4468–4472

Ladner HK, Led JJ, Grant DM (1975) Deuterium-isotope effects on ^{13}C chemical-ahifts in amino acids and dipeptides. J Magn Reson 20:530–534

Li YK, Kuliopulos A, Mildvan AS, Talalay P (1993) Environments and mechanistic roles of the tyrosine residues of delta-5-3-ketosteroid isomerase. Biochemistry 32:1816–1824

Liepinsh E, Otting G (1996) Proton exchange rates from amino acid side chains—implications for image contrast. Magn Reson Med 35:30–42

Liepinsh E, Otting G, Wüthrich K (1992) NMR spectroscopy of hydroxyl protons in aqueous solutions of peptides and proteins. J Biomol NMR 2:447–465

Liu YJ, Thoden JB, Kim J, Berger E, Gulick AM, Ruzicka FJ, Holden HM, Frey PA (1997) Mechanistic roles of tyrosine 149 and serine 124 in UDP-galactose 4-epimerase from *Escherichia coli*. Biochemistry 36:10675–10684

Löhr F, Rogov VV, Shi M, Bernhard F, Dötsch V (2005) Triple-resonance methods for complete resonance assignment of aromatic protons and directly bound heteronuclei in histidine and tryptophan residues. J Biomol NMR 32(4):309–328

Löhr F, Hansel R, Rogov VV, Dötsch V (2007) Improved pulse sequences for sequence specific assignment of aromatic proton resonances in proteins. J Biomol NMR 37(3):205–224

Lunin VV, Li YG, Linhardt RJ, Miyazono H, Kyogashima M, Kaneko T, Bell AW, Cygler M (2004) High resolution crystal structure of *Arthrobacter aurescens* chondroitin AC lyase: an enzyme-substrate complex defines the catalytic mechanism. J Mol Biol 337:367–386

McIntosh LP, Poon DKY, Schubert M, Au J, Okon M, Withers SG (2006) Unambiguous determination of the ionization state of a glycoside hydrolase active site lysine by ^{1}H-^{15}N heteronuclear correlation spectroscopy. J Am Chem Soc 128:15388–15389

McIntosh LP, Naito D, Baturin SJ, Okon M, Joshi MD, Nielsen JE (2011) Dissecting electrostatic interactions in *Bacillus circulans* xylanase through NMR-monitored pH titrations. J Biomol NMR (in press)

Miao SC, Ziser L, Aebersold R, Withers SG (1994) Identification of glutamic acid 78 as the active site nucleophile in *Bacillus subtilis* xylanase using electrospray tandem mass-spectrometry. Biochemistry 33:7027–7032

Nall BT, Zuniga EH (1990) Rates and energetics of tyrosine ring flips in yeast iso-2-cytochrome *c*. Biochemistry 29:7576–7584

Norton RS, Bradbury JH (1974) Carbon 13 nuclear magnetic resonance study of tyrosine titrations. J Chem Soc Chem Comm 870–871

Oldfield E, Norton RS, Allerhand A (1975a) Studies of individual carbon sites of proteins in solution by natural abundance carbon 13 nuclear magnetic resonance spectroscopy - relaxation behavior. J Biol Chem 250:6368–6380

Oldfield E, Norton RS, Allerhand A (1975b) Studies of individual carbon sites of proteins in solution by natural abundance carbon 13 nuclear magnetic resonance spectroscopy—strategies for assignments. J Biol Chem 250:6381–6402

Pace CN, Horn G, Hebert EJ, Bechert J, Shaw K, Urbanikova L, Scholtz JM, Sevcik J (2001) Tyrosine hydrogen bonds make a large contribution to protein stability. J Mol Biol 312:393–404

Pelton JG, Torchia DA, Meadow ND, Roseman S (1993) Tautomeric states of the active-site histidines of phosphorylated and unphosphorylated Iii(Glc), a signal-transducing protein from *Escherichia coli*, using 2-dimensional heteronuclear NMR techniques. Prot Sci 2:543–558

Plesniak LA, Connelly GP, Wakarchuk WW, McIntosh LP (1996a) Characterization of a buried neutral histidine residue in *Bacillus circulans* xylanase: NMR assignments, pH titration, and hydrogen exchange. Prot Sci 5:2319–2328

Plesniak LA, Wakarchuk WW, McIntosh LP (1996b) Secondary structure and NMR assignments of *Bacillus circulans* xylanase. Prot Sci 5:1118–1135

Prompers JJ, Groenewegen A, Hilbers CW, Pepermans HAM (1998) Two-dimensional NMR experiments for the assignment of aromatic side chains in ^{13}C-labeled proteins. J Magn Reson 130: 68–75

Rao DK, Bhuyan AK (2007) Complexity of aromatic ring-flip motions in proteins: Y97 ring dynamics in cytochrome c observed by cross-relaxation suppressed exchange NMR spectroscopy. J Biomol NMR 39(3):187–196

Richarz R, Wüthrich K (1978) Carbon-13 NMR chemical shifts of the common amino acid residues measured in aqueous solutions of linear tetrapeptides H-Gly-Gly-X-L-Ala-OH. Biopolymers 17: 2133–2141

Sattler M, Schleucher J, Griesinger C (1999) Heteronuclear multidimensional NMR experiments for the structure determination of proteins in solution employing pulsed field gradients. Prog Nucl Magn Reson Spect 34:93–158

Sidhu G, Withers SG, Nguyen NT, McIntosh LP, Ziser L, Brayer GD (1999) Sugar ring distortion in the glycosyl-enzyme intermediate of a family G/11 xylanase. Biochemistry 38:5346–5354

Skalicky JJ, Mills JL, Sharma S, Szyperski T (2001) Aromatic ring flipping in supercooled water: implications for NMR-based structural biology of proteins. J Am Chem Soc 123:388–397

Snyder GH, Rowan R, Karplus S, Sykes BD (1975) Complete tyrosine assignments in high field ^{1}H nuclear magnetic resonance spectrum of bovine pancreatic trypsin inhibitor. Biochemistry 14:3765–3777

Sun SX, Toney MD (1999) Evidence for a two-base mechanism involving tyrosine-265 from arginine-219 mutants of alanine racemase. Biochemistry 38:4058–4065

Sun XS, Sun HZ, Ge RG, Richter M, Woodworth RC, Mason AB, He QY (2004) The low pK_a value of iron-binding ligand Tyr188 and its implication in iron release and anion binding of human transferrin. FEBS Lett 573:181–185

Takeda M, Jee J, Ono AM, Terauchi T, Kainosho M (2009) Hydrogen exchange rate of tyrosine hydroxyl groups in proteins as studied by the deuterium isotope effect on C_ζ chemical shifts. J Am Chem Soc 131:18556–18562

Thurlkill RL, Grimsley GR, Scholtz JM, Pace CN (2006) pK values of the ionizable groups of proteins. Prot Sci 15:1214–1218

Ulrich EL, Akutsu H, Doreleijers JF, Harano Y, Ioannidis YE, Lin J, Livny M, Mading S, Maziuk D, Miller Z, Nakatani E, Schulte CF, Tolmie DE, Wenger RK, Yao HY, Markley JL (2008) BioMagResBank. Nucleic Acids Res 36:D402–D408

Wagner G (1980) Activation volumes for the rotational motion of interior aromatic rings in globular-proteins determined by high-resolution ^{1}H-NMR at variable pressure. FEBS Lett 112:280–284

Wagner G, Wüthrich K (1975) Proton NMR-Studies of aromatic residues in basic pancreatic trypsin inhibitor (BPTI). J Magn Reson 20:435–445

Wagner G, Wüthrich K (1978) Dynamic model of globular protein conformations based on NMR studies in solution. Nature 275: 247–248

Wagner G, Demarco A, Wüthrich K (1976) Dynamics of aromatic amino-acid residues in globular conformation of basic pancreatic

trypsin-inhibitor (BPTI). ^{1}H-NMR studies. Biophys Struct Mech 2:139–158

Wakarchuk WW, Campbell RL, Sung WL, Davoodi J, Yaguchi M (1994) Mutational and crystallographic analyses of the active site residues of the *Bacillus circulans* xylanase. Prot Sci 3:467–475

Watts AG, Damager I, Amaya ML, Buschiazzo A, Alzari P, Frasch AC, Withers SG (2003) *Trypanosoma cruzi* trans-sialidase operates through a covalent sialyl-enzyme intermediate: tyrosine is the catalytic nucleophile. J Am Chem Soc 125:7532–7533

Werner MH, Clore GM, Fisher CL, Fisher RJ, Trinh L, Shiloach J, Gronenborn AM (1997) Correction of the NMR structure of the ETS1/DNA complex. J Biomol NMR 10:317–328

Willard L, Ranjan A, Zhang H, Monzavi H, Boyko RF, Sykes BD, Wishart DS (2003) VADAR: a web server for quantitative evaluation of protein structure quality. Nucleic Acids Res 31: 3316–3319

Word JM, Lovell SC, Richardson JS, Richardson DC (1999) Asparagine and glutamine: using hydrogen atom contacts in the choice of side chain amide orientation. J Mol Biol 285: 1735–1747

Wüthrich K, Wagner G (1975) NMR investigations of dynamics of aromatic amino acid residues in basic pancreatic trypsin inhibitor. FEBS Lett 50:265–268

Yamazaki T, Forman-Kay JD, Kay LE (1993a) 2-Dimensional NMR experiments for correlating $^{13}C\beta$ and $^{1}H\delta/\varepsilon$ chemical-shifts of aromatic residues in ^{13}C-labeled proteins via scalar couplings. J Am Chem Soc 115:11054–11055

Yamazaki T, Yoshida M, Nagayama K (1993b) Complete assignments of magnetic resonances of ribonuclease H from *Escherichia coli* by double-resonance and triple-resonance 2D and 3D NMR spectroscopies. Biochemistry 32:5656–5669

Yamazaki T, Nicholson LK, Torchia DA, Wingfield P, Stahl SJ, Kaufman JD, Eyermann CJ, Hodge CN, Lam PYS, Ru Y, Jadhav PK, Chang CH, Weber PC (1994) NMR and X-ray evidence that the HIV protease catalytic aspartyl groups are protonated in the complex formed by the protease and a nonpeptide cyclic urea-based inhibitor. J Am Chem Soc 116:10791–10792

Yang W (2010) Topoisomerases and site-specific recombinases: similarities in structure and mechanism. Crit Rev Biochem Mol Biol 45:520–534

Zwahlen C, Legault P, Vincent SJF, Greenblatt J, Konrat R, Kay LE (1997) Methods for measurement of intermolecular NOEs by multinuclear NMR spectroscopy: application to a bacteriophage λ N-peptide/boxB RNA complex. J Am Chem Soc 119: 6711–6721